

Static behaviour of bolted shear connectors with mechanical coupler embedded in concrete

Branko Milosavljević^{*1}, Ivan Milićević^{1a}, Marko Pavlović^{2b} and Milan Spremić^{1c}

¹ Faculty of Civil Engineering, University of Belgrade, Bulevar kralja Aleksandra 73, 11000 Belgrade, Serbia

² Faculty of Civil Engineering and Geosciences, Delft University of Technology, Stevinweg 1, Delft, CD, Netherlands

(Received June 22, 2018, Revised September 4, 2018, Accepted September 12, 2018)

Abstract. The research of shear connectors composed from mechanical couplers with rebar anchors, embedded in concrete, and steel bolts, as a mean of shear transfer in composite connections is presented in the paper. Specific issues related to this type of connections are local concrete pressure in the connector vicinity as well as the shear flow along the connector axis. The experimental research included 18 specimens, arranged in 5 series. Nonlinear numerical analyses using Abaqus software was conducted on corresponding FE models. Different failure modes were analysed, with emphasis on concrete edge failure and bolt shear failure. The influence of key parameters on the behaviour of shear connector was examined: (1) concrete compression strength, (2) bolt tensile strength and diameter and (3) concrete edge distance. It is concluded that bolted shear connectors with mechanical couplers have sufficient capacity to be used as shear connectors in composite structures and that their behaviour is similar to the behaviour of post installed anchors as well as other types of connectors anchored without the head.

Keywords: steel-concrete composite structures; shear connectors; mechanical couplers; push-out tests, concrete edge breakout, finite element analysis

1. Introduction

Elements of shear connection in structures composed from reinforced concrete and steel members should be able to provide sufficient interaction to transfer shear forces and assure the composite action. Therefore, the behaviour of shear connection mostly depends on the applied type of shear connector. The most common connection of steel-concrete composite beams with in-situ casted concrete slab consists of welded headed studs continuously and uniformly distributed along beam length. Unlike, shear connectors of prefabricated steel-concrete composite structures are positioned between prefabricated or semi-prefabricated concrete slabs, interconnected by local in situ concreting. In such cases, various types of connectors are used: groups of welded headed studs or block type shear connectors. Assemblage of prefabricated concrete slabs and steel elements is also possible by casting bolts in concrete slab and predrilling flanges of the steel member.

A specific type of cast-in anchor is made out of two parts, as shown in Fig. 1(a). The first part consists of mechanical coupler and rebar anchor placed in formwork before concrete casting. After formwork removal, steel bolt is used as a second part of the assembly. The main purpose of these anchors is to provide adequate connection between

steel column and reinforced concrete foundation (Fig. 1(b)). In such cases, tension forces in bolts are transferred through mechanical coupler and rebar anchor to foundation. If this concept is applied for steel beam-concrete column connection (as shown in Fig. 1(c)) then the connector is dominantly loaded in shear. This type of shear connector can be used in building and bridge construction. In case of steel beam-concrete column connections, it simplifies the casting of concrete columns by enabling the use of continuous formwork. Furthermore, it can be used for prefabricated composite beams in buildings and bridges to ensure the reduction of construction time and enable dismantling.

According to CEB-FIP (2011), the common failure modes of shear connectors are steel (bolt) shear failure, pullout failure, pryout failure and concrete edge failure. The layout of shear connectors with rebar coupler (Fig. 1) shows that pullout failure cannot be expected, due to sufficient length of rebar anchor which provides adequate anchorage of the connector in concrete element. The way of anchoring also eliminates the possibility of pryout failure. Therefore, it can be concluded that possible failure modes of tested connectors with rebar coupler, which arise from specimen layout and load disposition, are steel (bolt) shear failure and/or concrete edge failure.

A review of literature indicates that very limited number of research work on bolted connectors with mechanical couplers is available. Yang *et al.* (2018) presented the performance of bolted connectors with similar layout as shown in Fig. 1 but instead of rebar anchor, the second (long) bolt was used. All specimens failed due to bolt shear failure with insignificant concrete damage and shear

*Corresponding author, Ph.D., Assistant Professor,
E-mail: brankom@imk.grf.bg.ac.rs

^a Ph.D. Student, E-mail: ivanm@imk.grf.bg.ac.rs

^b Ph.D., Assistant Professor

^c Ph.D., Assistant Professor

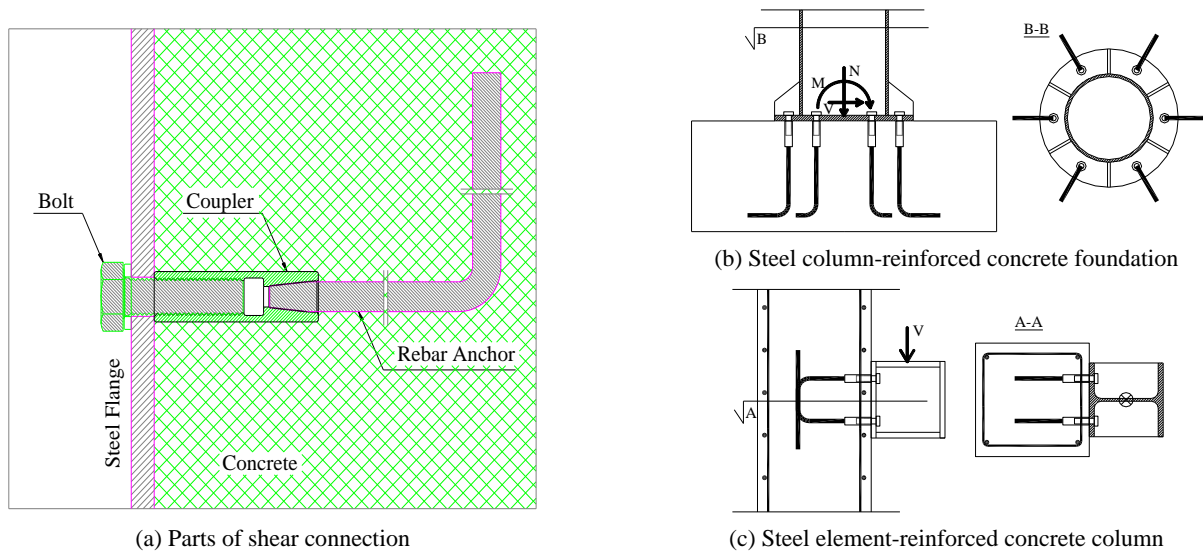


Fig. 1 Bolted connection with mechanical couplers

resistance being almost equal to corresponding welded stud connection. There is no explanation in the literature of the behaviour or failure modes of this type of shear connection beyond shear failure of bolts. In general, considering the layout of the connector, the behaviour and shear strength can be compared to bolted shear connectors with single or double embedded nut and post installed anchors with large embedment depth.

Considering the long period of application of welded headed studs in shear connections, research in this field, design recommendations and codes are by far the most numerous comparing to other types of shear connectors. Post installed anchors are more widely used over the past few decades, which is the reason for more extensive research of their behaviour in shear connections followed by scientific literature, design guides and codes of practice. There are few researches of bolted shear connectors in prefabricated composite structures, and recent findings pointed out the analogy with welded headed studs, which is the basis for the corrections of the behaviour model and design code provisions.

Ollgaard *et al.* (1971) conducted experimental research on 16 series of 3 specimens in push-out tests, in order to determine bearing capacity and force-slip curves of welded headed stud loaded in shear. Oehlers (1980) performed 79 push-out tests, with aim to determine the influence of key parameters on bearing capacity of welded studs loaded in shear. Very extensive state of the art is given by Pallarés and Hajjar (2010), based on comparison of 391 push-out test results of welded headed studs. Lam and El-Lobody (2005) built nonlinear FE model in addition to conducted experimental investigation of headed studs in push-out tests. Nguyen and Kim (2009) built 32 nonlinear numerical models of headed studs in push-out tests. Hällmark (2012) has published extensive study on composite bridges with prefabricated concrete slabs. The influence of reduced distances between studs on shear behaviour and strength was examined by Okada *et al.* (2006), Shim *et al.* (2008). Experimental and nonlinear numerical study of welded

headed studs arranged in groups was conducted by Spremić (2013).

In case of cast-in bolts, among the first to investigate the possibility of their application in shear connection between steel and reinforced concrete elements was Dallam (1968), who investigated high strength friction grip bolts. Marshall *et al.* (1971) also conducted research of friction grip bolts on standard push-out tests. Demountable shear connection with different details of the connection was analyzed by Lam *et al.* (2017). Bolted shear connections without embedded nut were investigated by Hawkins (1987) and Lam *et al.* (2013). Push-out tests on bolted shear connections with single embedded nut were first conducted by Dedic and Klaiber (1984). Among others, research on behaviour of bolted shear connectors was continued by Kwon (2008), who conducted single shear tests on bolts with double embedded nut. Very detailed study of bolted shear connection with single embedded nut in push-out tests was conducted by Pavlović *et al.* (2013). It included experimental tests as well as numerical analyses of this type of shear connection on nonlinear FE models in computer software Abaqus.

The researches of post installed anchors are very extensive and, in general, can be divided in two major groups: research of anchors loaded in tension and anchors loaded in shear. Apart from mechanical characteristics of used material, the main influence on the behaviour of anchors loaded in shear, perpendicular as well as parallel to the free edge, is concrete edge distance. Research of anchors loaded in shear was conducted by Grosser (2012). It contains a comprehensive state of the art on existing experimental and numerical results on post installed anchors and extensive experimental study. The research also included nonlinear numerical investigation as well as detail analysis of new concept of generating and transferring local stresses in concrete in case of anchors loaded in shear near concrete edge. It gives relatively simple and improved equations for calculation of anchor shear resistance comparing to equations given in current design codes.

Table 1 Specimen geometrical characteristics

Series	Num. of spec.	Concrete column dimensions			Bolts		Mechanical couplers		Rebar anchor	Sheer connector edge distance
		Base		Height	Diameter	Length	Diameter	Length	Diameter	
		b_c	d_c	h_c	D	L	d_{co}	L_{co}	d_s	
		mm	mm	mm	mm	mm	mm	mm	mm	
A	4	300	300	650	16	58	22	59	12	75
B	4	300	300	650	16	58	22	59	12	75
C	4	300	300	650	16	58	22	59	12	100
D	3	300	400	550	16	75	22	79	12	150
E	3	300	400	550	20	82	27	93	16	150

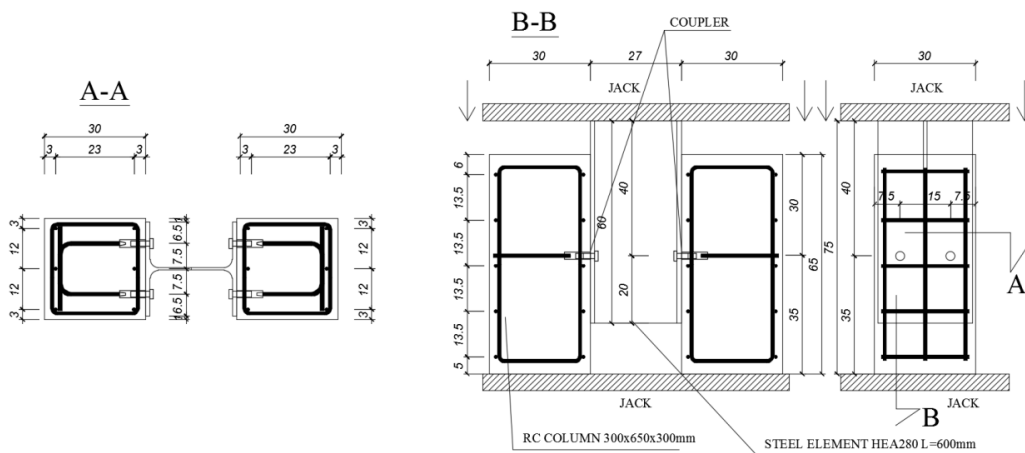


Fig. 2 Specimen layout series A with connector distance of 75 mm

This paper presents experimental results of 18 modified push-out tests of shear connectors with mechanical coupler under static shear load. The effects of key parameters on connector capacity and behaviour in push-out test were examined and discussed: concrete compressive strength, concrete edge distance, degree of confinement, bolt diameter and tensile strength. In order to evaluate the experimental results and explain failure modes of shear connection with mechanical coupler, advanced 3D nonlinear analysis of FE models of tested specimens is conducted in explicit software. The analysis is performed using damage plasticity models in Abaqus, with all parameters calibrated to experimental results. The numerical results are compared to test results in terms of ultimate shear resistance, ductility and failure modes.

2. Static experiments on connectors loaded in shear

Experimental research of reinforced concrete and steel element connection by rebar couplers was conducted in order to determine the load bearing capacity and behaviour of such connection under the static shear load, according to Eurocode 4 (2004). The testing was carried out in the Laboratory for Materials and Structures at the Faculty of Civil Engineering of the University of Belgrade.

2.1 Specimens for push-out tests

Tested specimens consist of two reinforced concrete prisms with one I-shaped steel element placed between them. The connection between steel and concrete elements was realised by shear connectors, consisting of steel bolts and built-in mechanical rebar couplers anchored by rebar (Fig. 2). The specimen layout was adopted in accordance to the test specimen for standard push test, as defined in Annex B of Eurocode 4 (2004), with certain alternation of concrete prism dimensions. Dimensions of concrete prisms were selected to relate to common column cross section dimensions in building structures, which are similar to those presented in test layout by Xue *et al.* (2012). All concrete columns were connected to the steel element using two shear connectors, giving four connectors per specimen. Experimental research included 18 specimens in total, arranged in 5 series. Specimen geometrical characteristics are given in Table 1.

All specimens included steel element HEA 280, 600 mm in length. Specimens from series A and B differ in the amount of transverse reinforcement (stirrups $\emptyset 8/135$ (A) and $\emptyset 10/110$, with reduction of stirrup spacing to $\emptyset 10/55$ in connection area (B)), in order to investigate the influence of more intensive confinement to concrete edge failure occurrence (and bearing capacity of concrete below the connector).



Fig. 3 Shear connector's attachment to the formwork

Table 2 Mechanical characteristics of tested concrete

Series	Testing age		Measured values			$f_{cm,cube}$	f_{cm}	f_{ctm}	E_{cm}	$f_{ctm}(t)$	$E_{cm}(t)$
	t		$f_{cm,cube}(t)$	$f_{ctm,sp}(t)$	$f_{ctm}^*(t)$						
	days		MPa	MPa	MPa						
A	28		33.60	-	-	33.60	26.60	2.106	29504	2.11	29504
B	15		30.96	-	-	33.93	26.86	2.126	29591	1.94	28789
C	15		43.48	2.30	2.07	47.65	37.72	2.879	32764	2.63	31877
D	12		36.07	2.36	2.12	41.15	32.58	2.536	31355	2.22	30139
E	10		42.07	2.59	2.33	49.78	39.41	2.987	33198	2.52	31563

The specimens casting was carried out in wooden formworks, with shear connector attached to the specimen formwork. The rectangular part of formwork bottom is constructed as demountable to enable multiple formwork use for specimens with different connector diameter or connector spacing and to ensure higher precision in connector installation (Fig. 3). All predrilled holes in the HEA 280 steel element are with diameter 1.0 mm greater than the bolt diameter, giving the bolt clearance randomly distributed in the interval from 0.0 to 1.0 mm. Considering that couplers are casted in precasted RC element, tolerance of ± 0.5 mm for assembling was adopted. After hardening, concrete columns were assembled to the steel element. The bolt load/torque applied was not measured, providing the small pretension, typical for non-preloaded bolts. Contact surfaces of each part of the connection were not greased in order to take into account friction forces between steel and concrete that occur in these connections in real structures.

2.2 Properties of the materials

Testing of material characteristic of specimen built-in materials was carried out using standard tests. Concrete, bolts, couplers and rebar anchors characteristics were tested. Testing of HEA element steel characteristics was not performed, due to low level of expected strain during push-out specimens testing.

The general intention in program of the experimental research was to form two groups of specimen, first with concrete edge failure occurrence (series A and B) and second, without (series C, D and E, with variation of connectors edge distance and bolt diameter). The higher concrete strength in second group was selected in order to avoid the concrete edge failure. Presented experimental

research was the base for forming calibrated numerical (FEA) model, which was, in further research, used for parametric analyses, with variation of concrete strength, connectors edge distance and bolt diameter.

Standard cube tests were used to determine compressive strength of concrete $f_{cm,cube}$ while cylinders tests were used to determine tensile strength of concrete, based on the splitting tensile strength $f_{ctm,sp}$. Test samples were cured in the same condition as concrete columns and were tested on the same day, as shown in Table 2. Measured values of strengths were used to determine mean values of cylinder compressive strength f_{cm} , tensile strength f_{ctm} and modulus of elasticity E_{cm} at 28 days according to Eurocode 2 (2004). Thus, this experimental research includes specimens prepared from "commercial" concrete with earlier connection loading, in accordance with the intention to model shear connections in real structures, considering concrete mixtures and possible connection assembling and loading prior to 28 days after casting.

Steel bolts, grade 8.8, were used in this research. Bolts were tested in three series, arranged by diameter and length for each specimen series, as specified in Table 1. Mechanical characteristics of tested bolts are presented in Table 3. Measured yield strength f_{02} , ultimate tensile strength f_{ub} and ultimate strain ϵ_u are shown.

Table 3 Mechanical characteristics of tested bolts

Series	Grade	Diameter	Length	f_{02}	f_{ub}	ϵ_u
		mm	mm	MPa	MPa	%
A, B, C	8.8	16	58	765.50	837.67	19.98
D	8.8	16	75	830.00	907.00	17.42
E	8.8	20	82	916.25	948.00	16.03

Table 4 Coupler mechanical characteristics

Series	Diameter	Length	R_{p02}	R_m	ϵ_u
	mm	mm	MPa	MPa	%
A, B, C	22	59	670.00	790.00	7.90
D	22	79	691.00	808.00	9.50
E	27	93	694.00	803.00	8.90

Mechanical couplers are arranged by diameter and length in three series which correspond to bolt diameters and lengths, as shown in Table 1. Testing results showed good match of tested mechanical characteristics with those specified by manufacturer. Coupler geometrical characteristic and nominal mechanical characteristics are presented in Table 4.

Testing results of rebar anchors $\emptyset 12$ and $\emptyset 16$, used for this research (Table 1), showed that measured mean values for yield strength f_{02} and tensile strength f_{ub} were 437.67 MPa and 605.33 MPa, respectively, with ultimate strain of 12.10%.

2.3 Test set-up

Specimen layout is presented on Fig. 4. All specimens were placed in hydraulic jack over a layer of fresh gypsum in order to ensure better support conditions and minimize the eccentricity effects. Vertical load was applied to the steel element using 3500 kN capacity hydraulic jack, in displacement control. It was applied in accordance to the loading procedure defined in Eurocode 4 (2004) – 25 load cycles in range from 5 to 40% of the expected ultimate load, with subsequent load increase up to specimen failure, in the time interval not shorter than 15 minutes. The expected ultimate load was determined as the total shear strength of 4 bolts, grade 8.8. Deformations were measured using LVDT (Linear Variable Displacement Transducer - 'HBM W A L') sensors (Fig. 4). Vertical slip between steel element and concrete column was measured at measuring points 1 to 4. Transversal separation between steel element and concrete columns was measured at points 5 and 6, while point 7 was used for measuring the transverse separation between two concrete columns.

2.4 Results of push-out experiments

All specimens were loaded until reaching the first bolt failure, corresponding to the ultimate load. After reaching the point of ultimate load, instant decrease of the measured load was recorded, indicating the test termination. The descending part of the presented force-slip diagrams in Fig. 5 was cut off at 90% of the ultimate load.

Key parameters that determine shear connection capacity and behaviour are ultimate force P_{ult} and ultimate slip δ_u . The ultimate slip δ_u is defined as a value of vertical slip measured from the end of cycling loading to the value of vertical slip corresponding to 90% of ultimate force, on descending part of the curve. The ultimate force and vertical slip for all specimen series are given in Table 5, with statistical evaluation of experimental results according to Eurocode 0 (Annex D). The ultimate slip is presented as averaged value for transducers 1-4 (Fig. 4). Force-slip curves for all 18 specimens are shown in Fig. 5.

2.4.1 Failure modes and damage patterns obtained in experiments

The results of experimental tests showed that bolt shear failure and crushing of concrete below the connector are common for all specimen series. However, a clear distinction can be made between two specimen groups regarding the behaviour and failure modes. The first group consists of specimen series A and B, with small concrete edge distance and relatively low concrete compressive strength f_{cm} (Table 6). The second group consists of specimen series C, D and E, with larger concrete edge distance and higher concrete strength.

Specimens in series A and B sustained characteristic concrete edge failure before reaching maximum measured force which corresponds to the bolt shear resistance, Fig. 6. Only specimen B2 failed due to concrete edge failure and extensive crushing of the compressed concrete below the connector without bolt shear failure, Fig. 7.

Concrete edge failure appears in the form of two inclined cracks that propagate from the connector to the concrete edge. Inclination angles below and above the connector, α and β respectively, are shown in Fig. 6. The values of angle α varied between 50° and 60° , while values

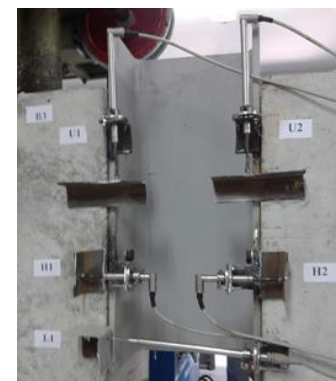
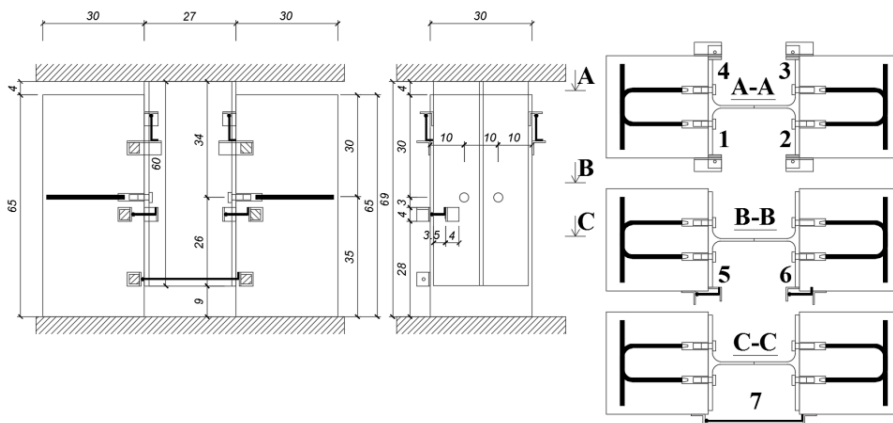


Fig. 4 Sensor layout

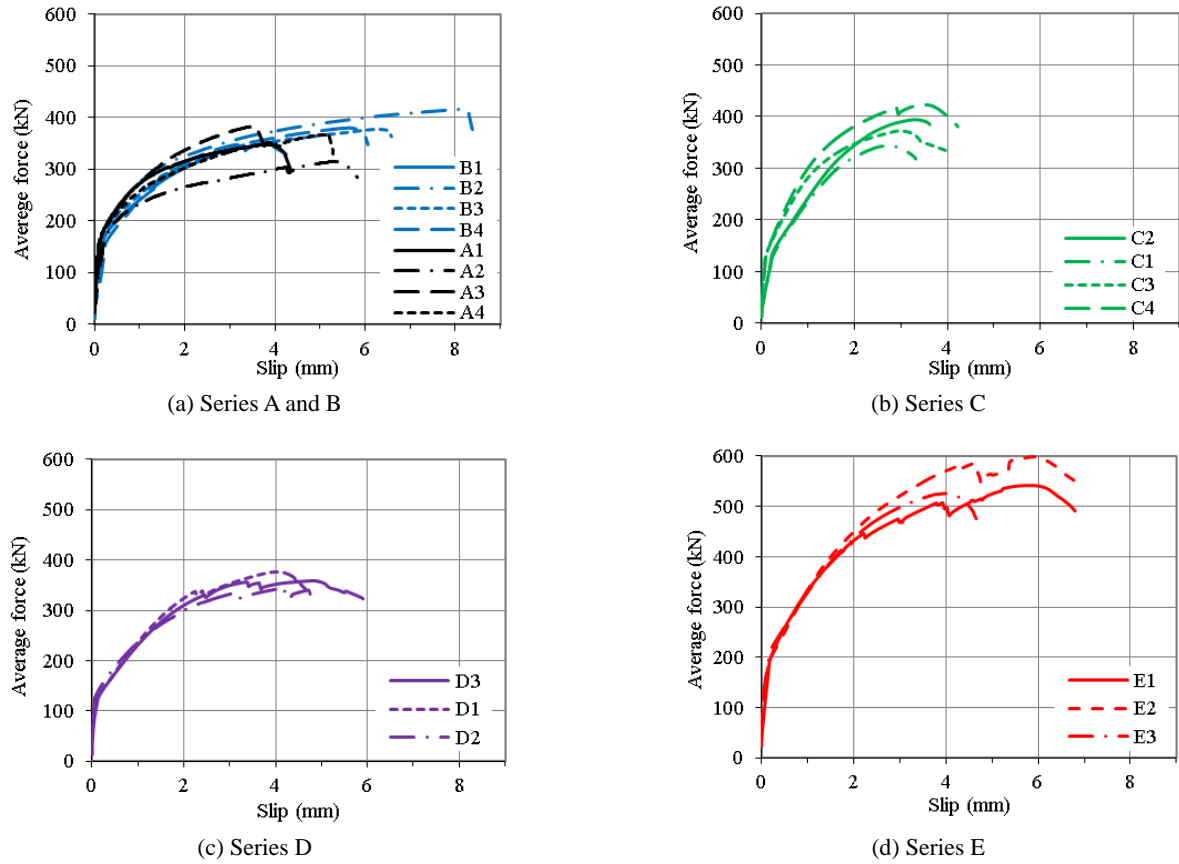


Fig. 5 Average force-slip behavior of coupler connectors embedded in concrete

Table 5 Ultimate forces and deformations

Series	Specimen	P_{ult} kN	$P_{ult,mean}$ kN	s_x	V_x (%)	$P_{ult,k}$ kN	δ_u mm	$\delta_{u,mean}$ mm	s_x	V_x (%)
A	A1	347.43					4.36			
	A2	314.35	353.10	29.62	8.39	275.20	5.82	4.82	0.92	19.19
	A3	382.78	366.01*	17.74*	4.85*	306.21*	3.77	4.48*	0.78*	17.45*
	A4	367.83					5.32			
B	B1	350.70					4.31			
	B2	415.95	381.05	26.78	7.03	310.64	8.59	6.47	1.79	27.63
	B3	337.80					6.94			
	B4	379.74					6.05			
C	C1	343.84					3.36			
	C2	394.23	383.34	33.57	8.76	295.06	3.71	3.81	0.37	9.71
	C3	372.23					3.96			
	C4	423.07					4.23			
D	D1	376.29					4.69			
	D2	343.78	359.64	16.27	4.52	324.70	5.08	5.22	0.62	11.88
	D3	358.84					5.90			
E	E1	541.92					7.20			
	E2	598.67	555.45	38.29	6.89	442.05	6.98	6.28	1.40	22.32
	E3	525.76					4.67			

* Calculated without taking into account A2 test results

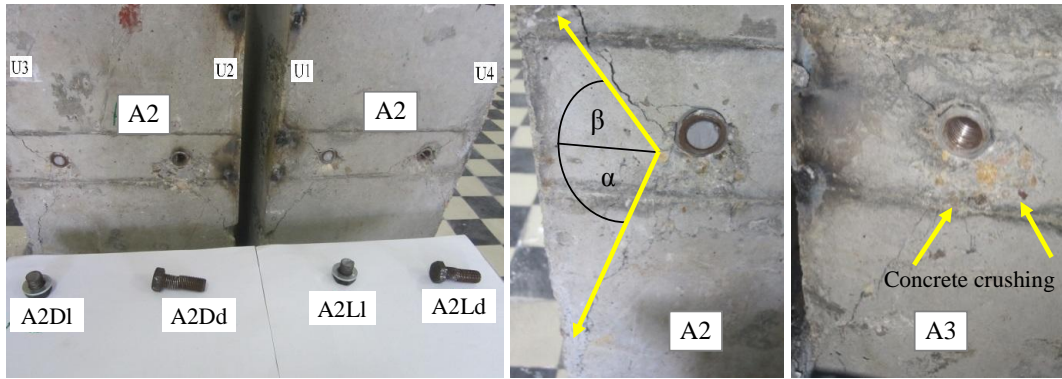


Fig. 6 Series A specimens after testing



Fig. 7 Series B specimens after testing

of β varied from 30° to 45° . Beside mentioned cracks, one horizontal crack between two connectors was also present. Similar crack pattern on concrete members with edge distance in range of 50-200 mm were detected and analysed by Grosser (2012). Values of the inclination angles α and β were around 75° and 65° , respectively. However, higher inclination angles and more severe damage of concrete members even for large edge distance detected by Grosser (2012) may be addressed to absence of reinforcement in tested members. Dai *et al.* (2015) have detected concrete edge damage on specimens with edge distance of $c = 100$ mm (equivalent to series C in this paper), but with lower concrete compressive strength (around 25 MPa). The degree of damage, related to concrete edge failure, was more pronounced on specimens A2 and A4 (crack width up to 1 mm) compared to A1 and A3 with smaller crack width (not wider than 0.3 mm). The inclined cracks with largest maximum crack width (up to 1.6 mm) were found on specimen B2. The inspection of the inner concrete was conducted, after removal of the damaged layer. It showed no visible damages on concrete core (confined by stirrups) in the connector vicinity, regardless of the degree of concrete edge damage which leads to a conclusion that concrete breakout body in both specimen series was only concrete cover deep.

The diagrams of vertical force as a function of transverse column to column separation (measured at point 7 according to sensor layout, Fig. 4) are presented for series A and B in Fig. 8. It is shown that transverse separations of concrete columns in series B are significantly larger than

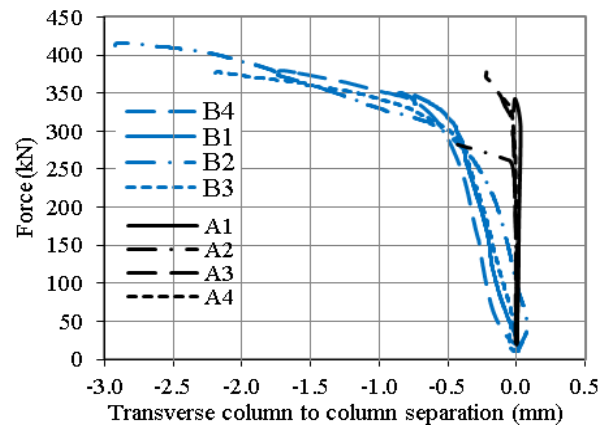


Fig. 8 Force-transverse column separation diagram for specimen series A and B

separations of columns in specimen series A. This clearly indicates that column support conditions were not identical which may be the main reason for more pronounced damage of specimens in series B in comparison to specimens in series A.

Specimens from series C, D and E failed due to bolt shear failure in one or two connectors. Tests showed that concrete edge failure did not occur, not even the presence of characteristic inclined cracks was spotted. Characteristic crushing of compressed concrete below the connectors of specimen C2 is shown in Fig. 9. Similar crushing patterns were detected on all other specimens in these three series.



Fig. 9 Specimen C2 after testing

2.4.2 Shear connection stiffness, resistance and ductility

Test results have shown that all series have similar behaviour in the elastic range, Fig. 5. High initial stiffness arises from the increased bearing surface provided by mechanical coupler. However, the influence of variation of key parameters (concrete compressive strength and coupler diameter) is compromised by different bolt-to-hole clearances within push-out specimens. The early onset of nonlinear behaviour is the result of thread penetration into the hole surface. Similar behaviour is detected by Pavlović *et al.* (2013), Pathirana *et al.* (2016) and Kwon (2008) for bolted connections with single and double embedded nut.

Mean values of measured ultimate shear connection resistance $P_{ult,mean}$ and maximum slip at failure $\delta_{u,mean}$ are presented for all specimen series in Table 6. No prediction equations for determining design shear resistance of shear connectors with mechanical coupler are given in Eurocode 4 (2004) or in any other design code. Therefore, characteristic value of bolt shear resistance $F_{v,Rk}$ given by Eq. (1), is calculated according to Eurocode 3 (2005) in order to evaluate experimental test results.

$$F_{v,Rk} = \alpha_v f_{ub} A_{net} \quad (1)$$

Shear resistance $F_{v,Rk}$ is adjusted to mean measured values of bolts strength f_{ub} for each specimen series, given in Table 3. Since the shear plane is passing through threaded portion of the bolts, tensile stress area of the bolts equal to 157 mm² and 245 mm² for M16 and M20, respectively, and $\alpha_v = 0.6$ were used. Values of shear resistance for four bolts are given in Table 6.

Series A and B specimens are characterized by typical concrete edge failure of anchors with sufficient anchorage length. They sustained concrete edge breakout before shear failure of one or more bolts. Concrete edge failure occurred at around 70% of the ultimate connection resistance – it is presented as stiffness reduction on the force-slip diagrams (Fig. 5). As a result of concrete damage, additional bearing capacity is achieved by rotation of the connector in the direction of applied force which induces catenary effects, as explained in Section 3.2.2. This is the main reason for increased shear resistance as opposed to pure shear (Table 6). It is believed that the amount of transverse reinforcement in this research did not affect shear resistance (approximately 4%) or ductility of the connection since concrete breakout body was limited to the concrete cover in both series. The effect of different horizontal stiffness of support layer (see Fig. 8) is more likely the reason for the

Table 6 Comparison of experimental results

Specimen series	Concrete edge distance	f_{cm} MPa	Diameter (f_{ub}) mm (MPa)	$P_{ult,mean}$ kN	Failure mode*	$\delta_{u,mean}$ mm	$4F_{v,Rk}$ kN	$P_{ult,mean}/4F_{v,Rk}$
	mm							
A	75	26.60	16 (837.67)	353.10 366.01**	CEF/BSF	4.82 4.48**	315.63	1.119 1.160**
B	75	26.86	16 (837.67)	381.05	CEF/BSF	6.47	315.63	1.207
C	100	37.72	16 (837.67)	383.34	BSF	3.81	315.63	1.215
D	150	32.58	16 (907.00)	359.64	BSF	5.22	341.76	1.044
E	150	39.41	20 (948.00)	555.45	BSF	6.28	557.42	0.996

* CEF = concrete edge failure, BSF = bolt shear failure

** Calculated without taking into account A2 test results

increase of series B connection slip (around 40% higher than connection slip of series A).

Failure mode of series C, D and E specimens was bolt shear failure which occurred without any sign of concrete damage near column edges. The higher $P_{ult,mean}/4F_{v,Rk}$ ratio of series C as opposed to series D and E (see Table 6) can be explained by the uncertainties related to the amount of friction in contact surfaces between steel member and concrete column. It is also the reason for 6.5% higher shear resistance of series C than series D in spite of higher bolt strength (see Table 6). On the other hand, connection slip of series C specimens is around 27% lower. The results show that ultimate resistance is increased by 54% with increase of bolt diameter from M16 (series D) to M20 (series E), for the same concrete edge distance. In addition, there is about 20% increase of the connection slip (see Table 6).

The ductility of tested connection can be assessed to the limit of $\delta_{uk} = 6$ mm, as per Eurocode 4 (2004). It is noticeable from Table 6 that only specimens from series B (characterized by extensive concrete edge failure) and series E (with M20 bolt connectors) meet this criterion. However, it should be noted that in both series some of mechanical couplers sustained cracking which increased the amount of connection slip, as explained in previous section. Therefore, the assumption of ideal plastic behaviour of shear connection with mechanical coupler is questionable which excludes their application in partial shear connection.

3. Numerical analysis

Numerical simulation of presented push-out specimens was conducted using Abaqus/Explicit solver which enabled fracture analysis with damage plastic models. Four different FE models of tested specimens were built – a single FE model for series A and B was used. The FE modelling included all parts of shear connector (bolts with washers, mechanical couplers and rebar anchors) with exact geometry as well as concrete columns and HEA steel element. The FEA models were calibrated based on the experimental test results, regarding all relevant characteristics: material properties, boundary conditions and load application. The calibration of parameters that were finally used for all FEA models was a complex task due to relatively large scatter in experimental test results. In order

to shorten the calculation time, one quarter of the push-out specimens was modelled using vertical symmetry boundary conditions, as shown in Fig. 10. The support point was fully restrained except in lateral (Z) direction, where restrain stiffness $k_{U3} = 40$ kN/mm was used to represent characteristics of the support gypsum layer. The restraining stiffness is calibrated using the results of multiple series of push-out experiments. A unique value is selected which ensures good match between the results of experiments and FEA for all series of specimens having different failure modes. This is done within larger set of results of push-out experiments than presented in this paper, see Pavlović *et al.* (2013) and Spremić *et al.* (2018).

Type and size of finite elements was chosen based on the geometry complexity of each part of the assembly and necessity to model complex localized stress and strain conditions in steel and concrete. Steel profile was modelled using hexahedral 8-node elements (C3D8R), 10 mm in size with densification to 0.5 mm elements in the vicinity of the hole. Tetrahedron elements (C3D4) were chosen for bolt, coupler, rebar and concrete parts. Bolt and mechanical coupler were modelled with 1.2 mm size elements, with densification to minimum dimension of 0.25 mm at bolt and coupler threads. Rebar anchor and reinforcement were modelled with 4.5 mm element size. Since the damage parameters of steel parts, described in Section 3.1.2, are dependent of mesh size, the size of the finite elements were adopted in calibration process based on the coupon test for bolts, couplers and rebar, see Pavlović and Veljković (2017) and Milosavljević (2014). Mesh size for concrete, with the dimensions in the interval from 4.4 to 11.5 mm, is a result of mesh size parametric study for shear force and vertical slip, see Fig. 11.

Contact interaction between two materials was defined in normal ("hard contact") and tangential direction ("penalty friction"). The friction coefficient between all the steel parts (coupler, bolt, washer, anchor) were set to value 0.3, except between the thread of the bolt and the coupler where coefficient of 0.14 was used as usual for the high strength bolts, see Pavlović *et al.* (2013). The interaction between steel parts (coupler, steel beam) and concrete slab was defined as contact interaction with friction coefficient 0.3, in accordance with ECCS (1985) recommendation. The interaction between the reinforcement bars and anchor were tie-constrained to the concrete slab. Friction coefficient

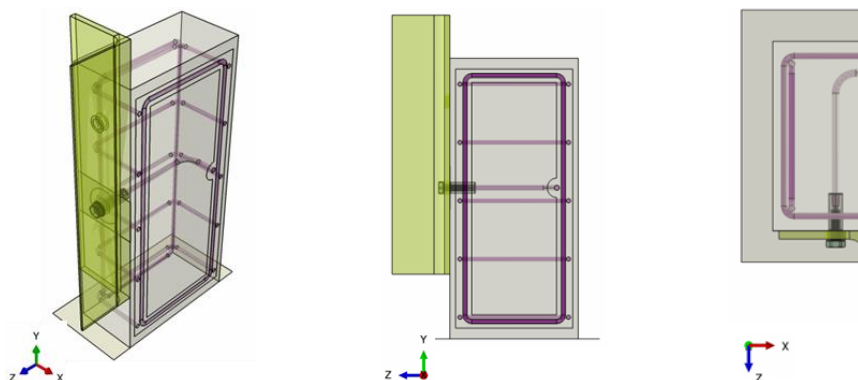


Fig. 10 FE model geometry

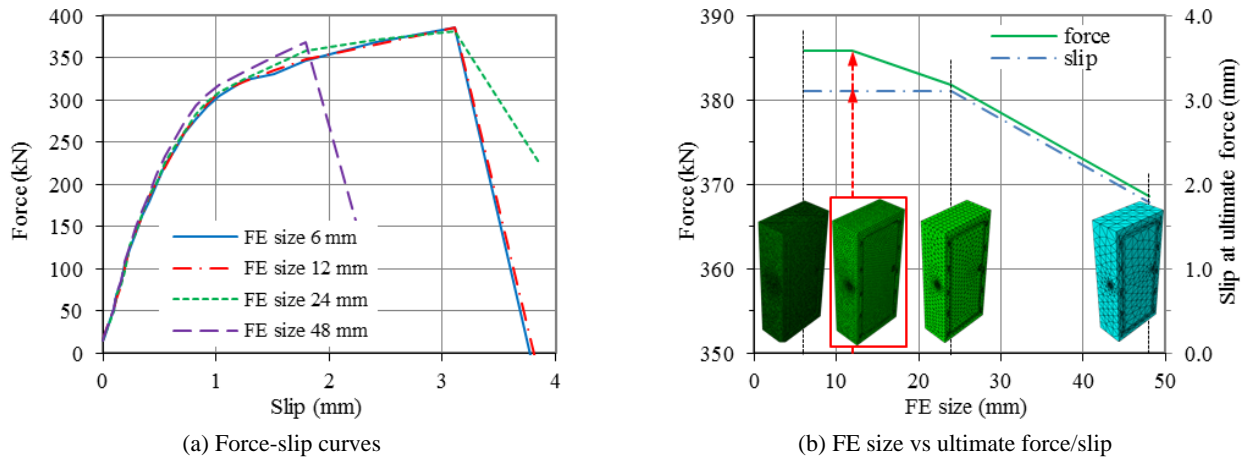


Fig. 11 Mesh sensitivity study for concrete parts – series C

between steel flange and concrete column was used since the friction between these two parts was not excluded by greasing.

Monotonic load was applied as displacement control at the top of steel profile, after the initial cyclic loading which corresponds to the first phase of experimental test procedure. Non-uniform mass scaling option combined with the time increment of 0.005 seconds was proved to be optimal. Bolts were not preloaded, which is consistent with assembling procedure of specimens in experimental tests. Bolt-to-hole clearance was adopted as ± 0.5 mm, as in experimental tests and bolts were positioned in the center of the hole. After the initial cycling loading, the bolt-to-hole clearance was closed.

3.1 Material models

Different material models in Abaqus have been defined for each part of the push-out tests FE model. Basic mechanical properties of the materials used in push-out tests were derived from standard material tests. Concrete, bolt and coupler mechanical properties are given in Tables 2, 3 and 4, respectively. Calibration of the plasticity and damage parameters of the material models for these parts was very important since the overall behaviour of the FEA push-out models highly depends on them.

3.1.1 Material model of concrete

Concrete damage plasticity (CDP) model was used to model the behavior of concrete part. The model includes

both compression and tension, defined by separate parameters. Measured values of concrete modulus of elasticity E_{cm} , compressive strength f_{cm} and tensile strength f_{ctm} are used for concrete material models, as presented in Table 7.

The FE simulation of concrete crushing observed in experimental tests has successfully been done by Xu *et al.* (2012), Pavlović *et al.* (2013) and Pathirana *et al.* (2016). The compressive stress-strain curve used in this paper is shown in Fig. 12. It was defined with two parts: (1) stress-strain curve according to Eurocode 2 (2004) up to the strain $\epsilon_{cu1} = 3.5 \cdot 10^{-3}$, and (2) the stress-strain curve proposed by Pavlović *et al.* (2013) as sinusoidal function with linear extension up to the maximal strain ϵ_{cuF} . After calibration, the following values of key parameters were adopted: the maximal strain $\epsilon_{cuF} = 0.10$ and corresponding remaining stress $f_{cuF} = 0.4$ MPa, curve slope parameters $\alpha_{tD} = 0.5$ and $\alpha_{tE} = 0.9$ as well as the stress reduction factor $\alpha = 15$ and corresponding strain $\epsilon_{cuE} = 0.03$. Spremić *et al.* (2018) used the same strain-stress curve with similar parameters for simulation of push-out tests on grouped headed studs.

Stress-strain curve for concrete in tension linearly increases until reaching concrete tensile strength f_{ctm} , with respect to modulus of elasticity. Crack opening and tension softening, characterized by descending part, lead to the decrease of tensile stress in sinusoidal manner to its minimum value $f_{ctF} = f_{ctm}/20$ with the maximal cracking strain $\epsilon_{ctF} = 0.001$ (Fig. 12).

The behaviour of concrete in triaxial compression was defined using the following plasticity parameters:

Table 7 Material characteristics adopted for FE modelling

Specimen	Measured values			FE model	Adopted values		
	f_{cm}	f_{ctm}	E_{cm}		f_{cm}	f_{ctm}	E_{cm}
	MPa	MPa	MPa		MPa	MPa	MPa
A	26.60	2.11	29504	FEM_A	27	2.1	29500
C	37.72	2.63	31877	FEM_C	38	2.6	32700
D	32.58	2.22	30139	FEM_D	32	2.2	31300
E	39.41	2.52	31563	FEM_E	40	2.5	33200

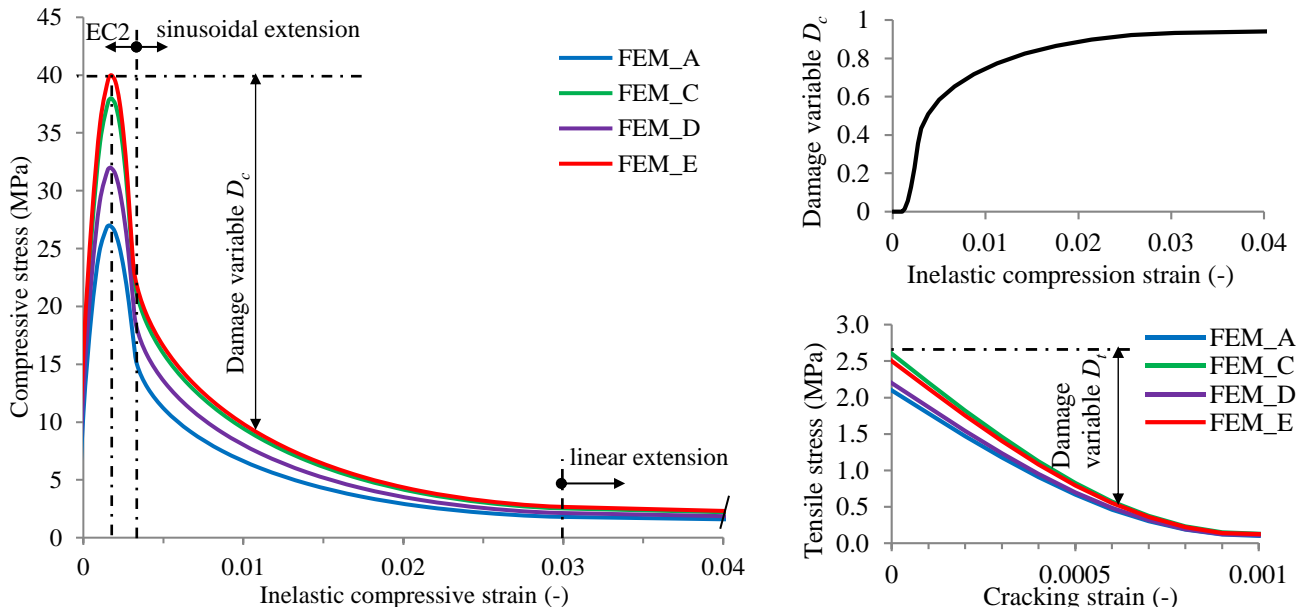


Fig. 12 Concrete stress-strain diagrams for FE modelling

- flow potential eccentricity e was set to 0.1, as recommended in Abaqus (2012);
- the biaxial-to-uniaxial compressive strength ratio was set to 1.2, as recommended by CEB-FIP Model code (1993);
- dilatation angle of $\psi = 36^\circ$ was adopted after calibration – similar value of $\psi = 38^\circ$ was recommended by Xu *et al.* (2012) and Jankowiak and Lodigowski (2005) while Spremić (2013) suggested that this value should be in the interval from 36° to 38° ;
- the ratio of yield stress in triaxial tension-to-compression was adopted as $K = 0.59$.

Damage evolution laws for concrete both in compression and tension were defined using two different damage variables: $D_c = 1 - f_{cm}/\sigma_c$ for compressive damage (presented in Fig. 12) and $D_t = 1 - f_{ct}/\sigma_t$ for tensile damage, which are based on corresponding inelastic strains.

3.1.2 Material models of steel parts

For material models of all steel parts of the connection

(bolt, mechanical coupler, rebar anchor and steel section) values of Poisson's ratio $\nu = 0.3$ and density $\gamma = 7850 \text{ kg/m}^3$ were adopted. Initial modulus of elasticity $E_0 = 195 \text{ GPa}$ was adopted for mechanical coupler (based on data provided by manufacturer) and $E_0 = 210 \text{ GPa}$ for all other steel elements.

Experimentally derived stress-strain curves for bolts and couplers were used for defining progressive damage models in Abaqus, which allowed presentation of failure modes and element removal in FE models. For bolts, as a part of the connector which is predominantly loaded in shear, both ductile and shear damage models were used. Unlike, only ductile damage model was defined for mechanical coupler and steel section.

The experimental results of standard tensile tests of built-in materials were used for defining damage evolution laws and stress-strain curves of parabolic shape, as presented in Fig. 13.

Considering the fact that the bolts were predominantly loaded in shear, parameters of shear damage were defined to match experimental results. Shear damage initiation criterion is determined as function of shear stress ratio θ_s .

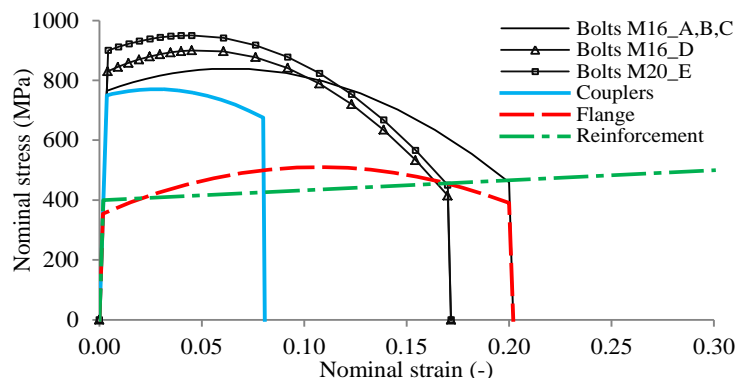


Fig. 13 Material models for steel components of the connection

Table 8 FE analysis vs. experimental test results

Specimen	Experimental results		FE model	Numerical results		Comparison	
	$P_{ult,exp}$ kN	$\delta_{u,exp}$ mm		$P_{ult,FEM}$ kN	$\delta_{u,FEM}$ mm	$P_{u,FEM}/P_{u,exp}$	$\delta_{u,FEM}/\delta_{u,exp}$
A+B	374.60*	5.62*	FEM_A	393.60	4.94	1.05	0.88
C	383.34	3.81	FEM_C	385.90	3.18	1.01	0.83
D	359.64	5.22	FEM_D	381.70	4.36	1.06	0.84
E	555.45	6.28	FEM_E	592.40	4.99	1.07	0.79

* Calculated without taking into account A2 test results

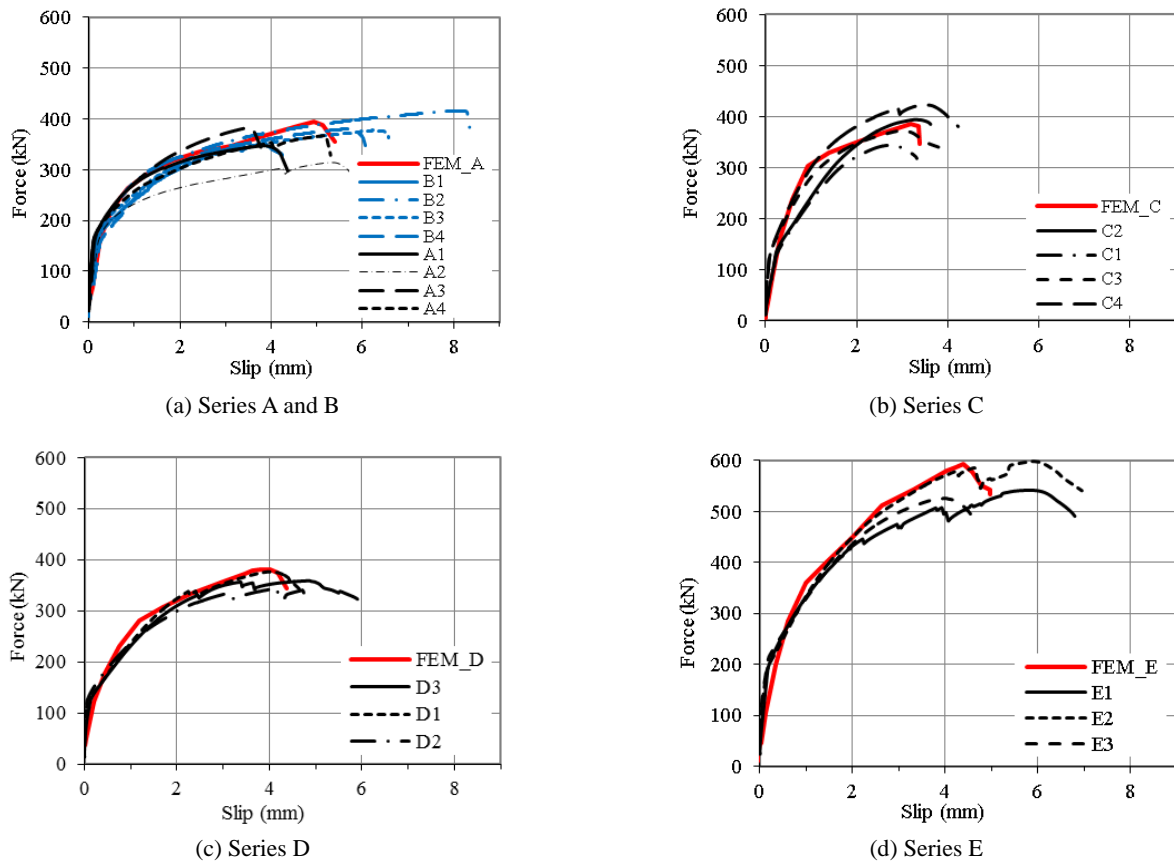


Fig. 14 Experimental and FE model force-slip curves

(Pavlović *et al.* (2013)) calibrated the values of shear damage material model by comparing experimental shear test of the bolt and corresponding FE model. It was concluded that the value of the shear-stress ratio does not significantly differ from the value for pure shear condition ($\theta_s = 1.732$). Therefore, shear damage initiation was set to constant value of equivalent plastic strain $\bar{\epsilon}_s^{pl} = 0.05$, corresponding to the onset of damage rather than as a function of θ_s . Shear damage evolution law with exponential softening is defined with the plastic strain at the onset of damage $\bar{\epsilon}_s^{pl}$ and maximal plastic deformation $\bar{u}_{f,s}^{pl} = 2.0$ mm, with exponential law parameter of 0.7.

Mechanical coupler steel characteristics were defined through synthetic, nominal stress-strain diagram with yield strength $R_{p02} = 750$ MPa, tension strength $R_m = 770$ MPa

and maximal strain $\epsilon_{uz} = 8\%$ (Fig. 13). In accordance with coupler stress mode, only ductile damage material model was used.

Steel section flange material model was defined with synthetic stress-strain diagram based on the assumption, with nominal yield strength $R_{p02} = 355$ MPa, tension strength $R_m = 510$ MPa and maximal strain $\epsilon_m = 20\%$, provided by manufacturer. Rebar anchors were modelled by bilinear diagrams with $R_{p02} = 400$ MPa and $R_m = 500$ MPa.

3.2 FEA results and validation vs. experiments

In order to validate FEA models, the vertical force-slip curves for the FEA models are presented in Fig. 14 with the corresponding curves obtained from experimental research for each specimen series. The numerical analysis results

showed good agreement with experimental test results, especially in terms of shear resistance and stiffness. It can be noticed from Table 8 that differences between ultimate force values obtained from FE analysis and experimental research are in the range from 1% to 7%. In addition to concrete failure mode, uncertainties, mostly related to friction effects and crack occurrence on coupler walls, led to larger differences between compared values of maximal vertical slip, in range from 13% to 20%. Nevertheless, because of high variation coefficients of experimentally obtained values for both ultimate force and vertical slip (presented in Table 5), the differences in this range can be considered reasonably accurate for further analyses of stress and strain distribution in the connector and its vicinity as well as failure modes and material damages.

3.2.1 Concrete damages

The FEA models simulated failure modes of corresponding push-out specimens rather correctly, regarding concrete crushing in front of the connector and concrete edge breakout, which are shown on Figs. 15-16. On all tested specimens, in the scope of experimental research, damages on the compressed concrete in front of

the connector were observed, to a greater or lesser extent. They appeared in form of spalling or breaking of the concrete cover at interface surfaces with steel flanges, as a result of reaching compression concrete strength in triaxial stress state. The comparison of concrete crushing patterns observed on test specimen A and corresponding FE analysis results, shown as concrete compressive damage variable (DAMAGEC), is presented in Fig. 15(a). It is evident that the degree and area of concrete damage on FEA models match those detected on test specimens. Furthermore, FE analysis showed that high crushing and overall damage of concrete that occur in the vicinity of shear connector are limited only concrete cover while inner concrete core confined by stirrups remains undamaged, as shown in Fig. 15(b).

In order to detect crack initiation and damage development in concrete edge vicinity, lateral displacement of concrete edge from the connector axes was recorded and presented as a function of applied vertical force in Fig. 16(a). It shows that lateral displacements of FE models FEM_C, FEM_D and FEM_E are negligible which corresponds to the experimental test results of those specimen series, since no inclined cracks were observed

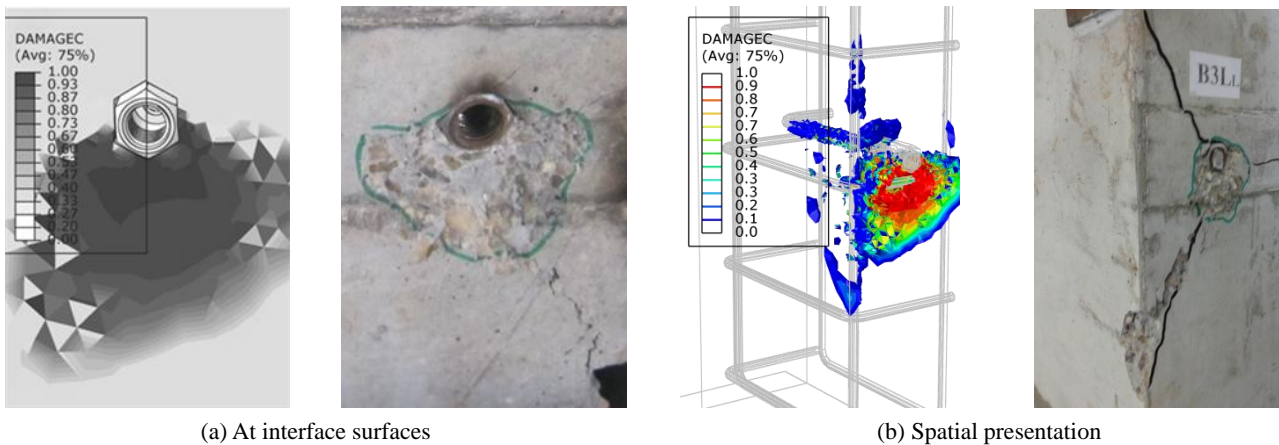
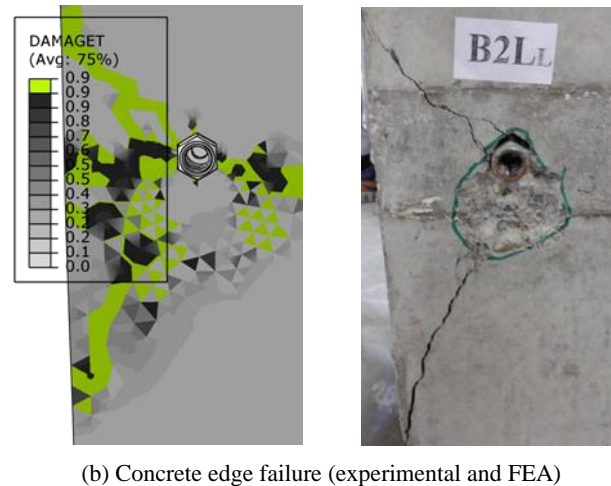
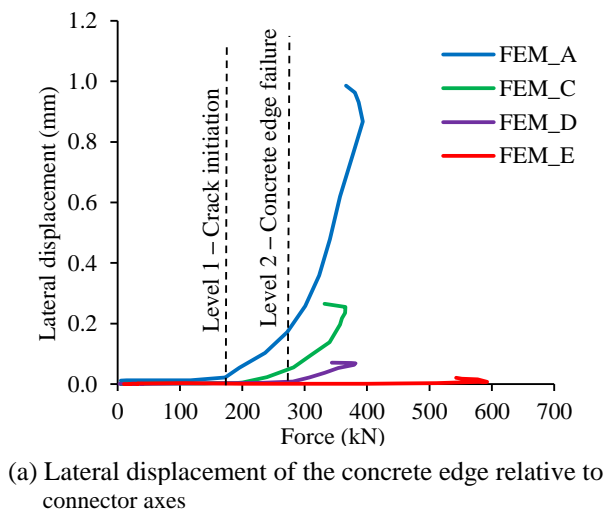


Fig. 15 Concrete crushing (experimental and FEA)



(a) Lateral displacement of the concrete edge relative to connector axes

(b) Concrete edge failure (experimental and FEA)

Fig. 16 Concrete edge failure

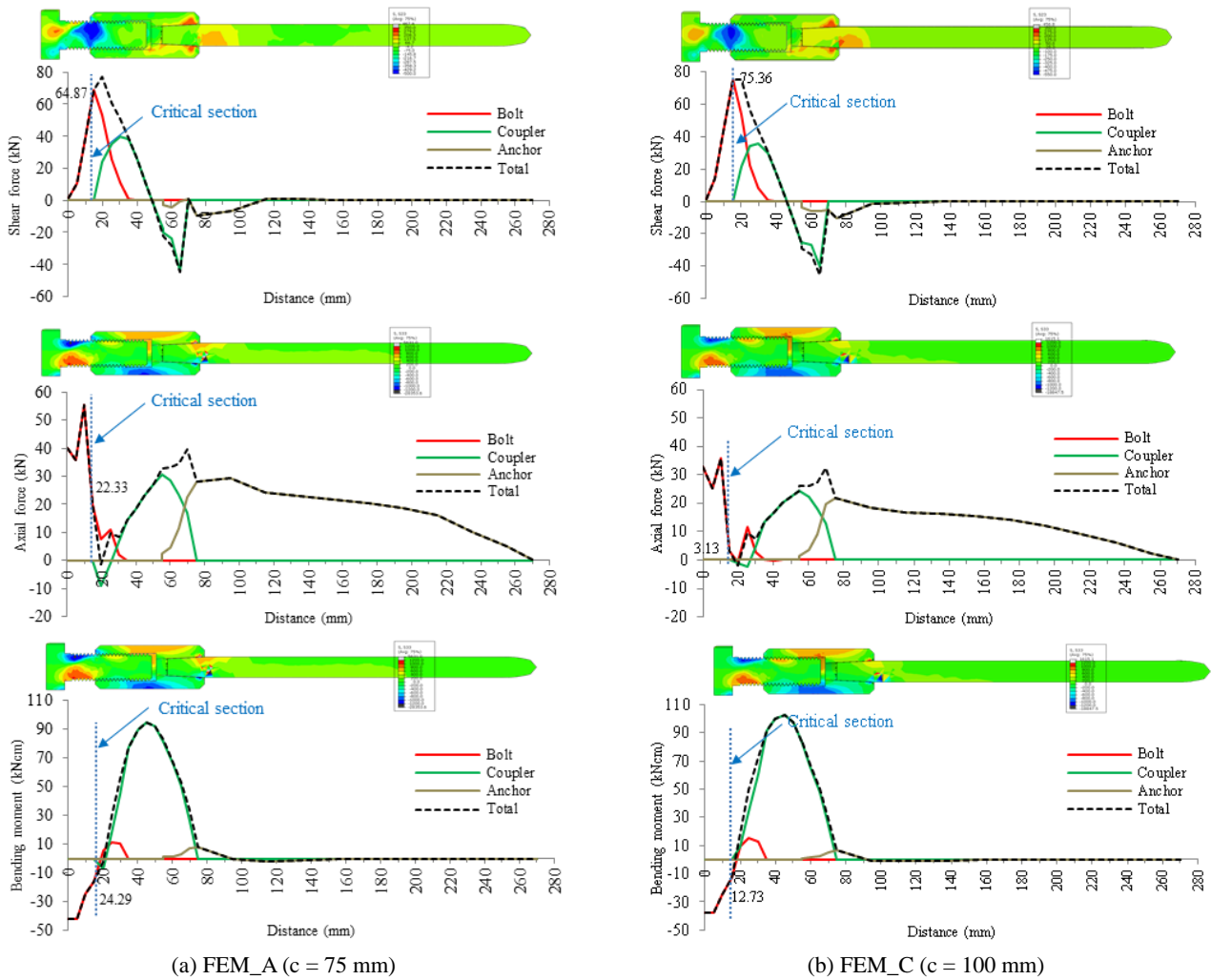


Fig. 17 Internal forces in shear connector

(Section 2.4). On the other hand, significant lateral displacements presented for FEM_A are developing from inclined crack initiation (force level 1) to concrete edge failure – full development of inclined cracks (force level 2). Fig. 16(b) displays characteristic inclined cracks from the connector to the concrete edge found in series B specimen and corresponding FEM_A evaluation, presented as concrete tension damage variable (DAMAGET).

3.2.2 Failure modes of the shear connector

As noted in Sections 2.4.1 and 2.4.2, almost all series failed due to bolts shear failure. However, there is significant difference between two specimen groups regarding behaviour and failure modes. The main reason is smaller edge distance of shear connectors from concrete edge used in series A and B in comparison to edge distance used in series C, D and E (Table 6). It is related to the degree of concrete damage and vertical slip of the connection.

In order to investigate failure modes of shear connector as a function of concrete edge distance, internal forces distributions prior to failure, in shear connector and all of its parts, are compared for FEM_A and FEM_C, as shown in

Fig. 17. Internal forces – shear force, axial force and bending moment are obtained by the integration of transversal (S23) and longitudinal (S33) stresses in connector elements. The connectors are presented in undeformed shape.

Fig. 17 shows that the failure of specimens with larger edge distance, FEM_C, is governed by shear failure of bolts with small contribution of the bending moment and axial force. The degree of concrete damage of FEM_C is also small (Fig. 16(a)). Unlike, the degree of concrete damage and connection slip at failure in FEM_A are larger leading to connector's rotation in the direction of applied vertical force. This behavior implies significantly higher axial tensile force in shear connector (Fig. 17(a)) due to catenary effects. In this case, more ductile failure mode of the bolt is exhibited due to combination of shear, tension and bending, resulting in increased shear resistance. Similar failure mechanism was described by Pavlović *et al.* (2013) on bolted shear connections with single embedded nut.

4. Conclusions

The behaviour of shear connector with coupler with

rebar tail embedded in concrete is investigated by conducting push-out tests in accordance with Eurocode 4 (2004). Eighteen push-out test specimens were arranged in five series, which differ in most influencing parameters: concrete compressive strength, concrete edge distance, degree of confinement, bolt diameter and tensile strength. The push-out tests were simulated using FE models where damage of all the materials are accurately modelled. Based on experiment and FE results failure modes of the connection are analyzed and following conclusions are drawn:

- Shear connectors with rebar mechanical coupler are suitable for use in steel to concrete connections predominantly loaded in shear, considering their strength and ultimate deformation, as well as their behaviour under increasing load.
- Specimens with small edge distance ($c = 75$ mm) and lower concrete strength exhibit concrete edge failure before shear failure of the bolts. Unlike, specimens with large edge distance ($c = 100$ - 150 mm) and higher concrete strength failed due to bolt shear failure only.
- Specimens with small concrete edge distance ($c = 75$ mm) and low concrete strength showed around 50% larger nonlinear displacement and ductility compared to specimens with larger concrete edge distance ($c = 100$ mm).
- The increase of edge distance from 100 mm to 150 mm did not affect shear resistance of the connection. However, there is around 37% increase of connection slip.
- The results show that ultimate resistance is increased by 54% with increase of bolt diameter from M16 to M20 for the same concrete edge distance ($c = 150$ mm). In addition, there is about 20% increase of the connection slip, leading to slip larger than 6 mm which is minimum requirement for non-brittle shear connection according to Eurocode 4.
- In-depth analysis of failure modes using validated FEA results showed that specimens with small concrete edge distance show more ductile behavior and relatively increased shear resistance due to catenary effects which arise from connector's rotation in the direction of applied vertical force.

Acknowledgments

The research described in this paper was supported by the Serbian Ministry of Education, Science and Technological Development through the TR-36048 project.

References

CEB-FIP Model code (1993), Design of concrete structures, CEB-FIP model code 1990; Thomas Telford; London, UK.
 CEB-FIP (2011), Design of Anchorages in Concrete (fib Bulletin 58), International Federation for Structural Concrete (fib); Lausanne, Switzerland.

Dallam L.N. (1968), "High strength bolts shear connectors – pushout tests", *ACI J. Proc.*, **65**(9), 767-769.
 Dedic, D.J. and Klaiber, W.F. (1984), "High-strength bolts as shear connectors in rehabilitation work", *Concrete Int.*, **6**(7), 41-46.
 Dai, X.H., Lam, D. and Saveri, E. (2015), "Effect of concrete strength and stud collar size to shear capacity of demountable shear connectors", *J. Struct. Eng.*, **141**(11), 04015025, 1-10.
 ECCS (1985), ECCS Publication No 38 - European Recommendations for Bolted Connections in structural steelwork, ECCS, Brussels, Belgium.
 Eurocode 0 (2002), Basis of structural design, European Committee for Standardization (CEN); Brussels, Belgium.
 Eurocode 2 (2004), Design of concrete structures. Part 1.1: General rules and rules for buildings, European Committee for Standardization (CEN); Brussels, Belgium.
 Eurocode 3 (2005), Design of steel structures. Part 1.8: Design of joints, European Committee for Standardization (CEN); Brussels, Belgium.
 Eurocode 4 (2004), Design of composite steel and concrete structures. Part 1.1: General rules and rules for buildings, European Committee for Standardization (CEN); Brussels, Belgium.
 Hällmark R. (2012), "Prefabricated composite bridges – a study of dry deck joints", Licentiate Thesis; Luleå University of Technology, Luleå, Sweden.
 Hawkins, N. (1987), "Strength in shear and tension of cast-in-place anchor bolts", *Anchorage Concrete*, SP-103, 233-255.
 Grosser, P. (2012), "Load-bearing behavior and design of anchorages subjected to shear and torsion loading in uncracked concrete", Ph.D. Dissertation; Institut für Werkstoffe im Bauwesen der Universität Stuttgart, Stuttgart, Germany.
 Jankowiak, T. and Lodigowski, T. (2005), "Identification of parameters of concrete damage plasticity constitutive model", *Found. Civil Environ. Eng.*, **6**(1), 53-69.
 Kwon, G. (2008), "Strengthening existing steel bridge girders by the use of post-installed shear connectors", Ph.D. Dissertation; The University of Texas at Austin, Austin, TX, USA.
 Lam, D. and El-Lobody, E. (2005), "Behavior of headed stud shear connectors in composite beam", *J. Struct. Eng.*, **131**(1), 96-108.
 Lam, D., Dai, X. and Saveri, E. (2013), "Behaviour of demountable shear connectors in steel-concrete composite beams", *Proceedings of the 7th International Conference on Composite Construction in Steel and Concrete*, Palm Cove, Australia, July.
 Lam, D., Dai, X., Ashour, A. and Rahman, N. (2017), "Recent research on composite beams with demountable shear connectors", *Steel Constr. Des. Res.*, **10**(2), 125-134.
 Marshall, W.T., Nelson, H.M. and Banerjee, H.K. (1971), "An experimental study of the use of high-strength friction-grip bolts as shear connectors in composite beams", *Struct. Eng.*, **49**(4), 171-178.
 Milosavljević B. (2014), "Theoretical and experimental research of the behaviour of reinforced concrete and steel element connection by rebar couplers", Ph.D. Dissertation; University of Belgrade, Belgrade, Serbia.
 Nguyen H.T. and Kim, S.E. (2009), "Finite element modelling of push-out tests for large stud shear connectors", *J. Constr. Steel Res.*, **65**(10-11), 1909-1920.
 Oehlers, D.J. (1980), "Stud shear connectors for composite beams", Ph.D. Dissertation; University of Warwick, Coventry CV4 7AL, UK.
 Okada J., Teruhiko, Y. and Lebet, J.P. (2006), "A study of the grouped arrangements of stud connectors on shear strength behaviour", *Struct. Eng./Earthq. Eng.*, **23**(1), 75s-89s.
 Ollgaard, J.G., Slutter, R.G. and Fisher, J.W. (1971), "Shear strength of stud connectors in lightweight and normalweight concrete", *Eng. J. Amer. Inst. Steel Constr.*, **8**(2), 55-64.

- Pallarés L. and Hajjar, J.F. (2010), "Headed steel stud anchors in composite structures, part I: shear", *J. Constr. Steel Res.*, **66**(2), 198-212.
- Pathirana, S.W., Uy, B., Mirza, O. and Zhu, X. (2016), "Bolted and welded connectors for rehabilitation of composite beams", *J. Constr. Steel Res.*, **125**, 61-73.
- Pavlović, M., Marković, Z., Veljković, M. and Budjevac, D. (2013), "Bolted shear connectors vs. headed studs behaviour in push-out tests", *J. Constr. Steel Res.*, **88**, 134-149.
- Pavlović, M. and Veljković, M. (2017), "FE validation of push-out tests", *Steel Constr. Des. Res.*, **10**(2), 135-144.
- Shim, C.S., Lee, P.G., Kim, D.W. and Chung, C.H. (2008), "Effects of group arrangement on the ultimate strength of stud shear connection", *Proceedings of the 6th International Conference on Composite Construction in Steel and Concrete*, Tabernash, CO, USA, July.
- Spremić, M. (2013), "The analysis of headed studs group behavior in composite steel-concrete beam", Ph.D. Dissertation; University of Belgrade, Belgrade, Serbia.
- Spremić, M., Pavlović, M., Marković, Z., Veljković, M. and Budjevac, D. (2018), "FE validation of the equivalent diameter calculation model for grouped headed studs", *Steel Compos. Struct., Int. J.*, **26**(3), 375-386.
- Xu, C., Sugiura, K., Wu, C. and Su, Q. (2012), "Parametrical static analysis on group studs with typical push-out tests", *J. Constr. Steel Res.*, **72**, 84-96.
- Xue, D., Liu, Y., Yu, Z. and He, J. (2012), "Static behavior of multi-stud shear connectors for steel-concrete composite bridge", *J. Constr. Steel Res.*, **74**, 1-7.
- Yang, F., Liu, Y., Jiang, Z. and Xin, H. (2018), "Shear performance of a novel demountable steel-concrete bolted connector under static push-out tests", *Eng. Struct.*, **160**, 133-146.